

Design of a Coplanar Integrated Microstrip Antenna for GPS/ITS Applications

Kunpeng Wei, Zhijun Zhang, *Senior Member, IEEE*, and Zhenghe Feng, *Senior Member, IEEE*

Abstract—This letter presents a novel low-profile coplanar multifunctional microstrip antenna for both global positioning system (GPS) and intelligent transportation system (ITS) applications. The multifunctional antenna consists of two parts: a directional coupled square-ring patch antenna and a center-fed square-ring loaded patch antenna. A coplanar simple single-fed method is proposed in the directional coupled square-ring patch antenna, which operates at the fundamental TM_{11} mode with right-handed circular polarization at the GPS L2 frequency of 1.227 GHz. Moreover, the square-ring is also utilized to load the center-fed square patch antenna at TM_{02} mode with a vertical linear polarization for ITS application, which considerably increases the impedance bandwidth. Very good consistency between the measurement and simulation for the return loss and radiation patterns is achieved.

Index Terms—Dual polarization, microstrip antennas, multifunctional, square-ring.

I. INTRODUCTION

DUE TO the rapid development of wireless communication systems, various services have been indispensable in modern life and integrated to collaborate with each other. In order to improve the utility efficiency of the limited spectra and spatial resources, different services using the same antenna are required. Because of the requirements with different radiation and polarization performances for different applications, conventional single-fed multiband antennas [1] are not practical. Hence, the multifunctional antenna with different radiation characteristics has become more and more important for antenna designers. A representative example is the use of one multifunctional antenna in a vehicle to produce both a broadside circularly polarized pattern for satellite-positioning application and an omni-azimuthal radiation pattern for terrestrial mobile communication service [2]. The reason is that many terrestrial wireless communication applications should be location-based or require knowledge of vehicle location, which could be achieved through the use of Global Positioning System (GPS).

Manuscript received December 20, 2010; revised February 28, 2011 and April 06, 2011; accepted April 19, 2011. Date of publication May 19, 2011; date of current version May 26, 2011. This work was supported in part by the National Basic Research Program of China under Contract 2009CB320205, the National High Technology Research and Development Program of China (863 Program) under Contract 2007AA01Z284, the National Natural Science Foundation of China under Contract 60771009, and the National Science and Technology Major Project of the Ministry of Science and Technology of China 2010ZX03007-001-01.

The authors are with the State Key Lab of Microwave and Communications, Department of Electronic Engineering, Tsinghua University, Beijing 100084, China (e-mail: zjzh@tsinghua.edu.cn).

Color versions of one or more of the figures in this letter are available online at <http://ieeexplore.ieee.org>.

Digital Object Identifier 10.1109/LAWP.2011.2152361

Intelligent transport systems (ITS) adopt traveling information in moving vehicles over highways to improve the transport safety and reduce environmental impact. In China and the U.S., the 5.8-GHz frequency band has been assigned for ITS-dedicated short-range communication service (DSRCS) [3]. In the U.K., emerging 4G high-performance unlicensed (free service) 5.470–5.725 GHz band Worldwide Interoperability for Microwave Access (WiMAX) mobile technology IEEE 802.16e has been considered as a potential candidate for use in ITS [4]. As mentioned, GPS is usually integrated to collaborate with the terrestrial ITS service. Furthermore, according to IEEE communication standards, time synchronization obtained by GPS is required for ITS services. Therefore, the automotive market requires compact, high-performance, and cheap solutions that accommodate GPS/ITS services with the smallest volume mounted on the roof of a vehicle. In [5], a collocated dual-feed microstrip antenna for integrated GPS/ITS operation has been presented. However, due to the large size and poor impedance matching, the four-layer structure is difficult to employ.

In this letter, we present a coplanar integrated microstrip antenna solution for GPS and ITS services constrained within a volume of $55 \times 55 \times 3 \text{ mm}^3$, which is about 40% less than the electrical size of the antenna in [5]. The design is being developed to satisfy not only 5.8-GHz DSRCS band and other adjacent potential bands (unlicensed) for ITS service, but also the right-handed circularly polarized (RHCP) signal at 1.227 GHz (L2 Band) with regard to GPS service. The geometry of the proposed GPS/ITS multifunctional antenna employs only a single dielectric layer, which is easy to fabricate and assemble in compliance with the space limitation requirements of the automotive market.

II. ANTENNA DESIGN

The basic geometry of the proposed antenna GPS/ITS integrated antenna is shown in Fig. 1. The multifunctional antenna must simultaneously support GPS/L2 with right-handed circular polarization at 1.27 GHz and ITS 5.8-GHz frequency band with vertical polarized omnidirectional pattern. The design mainly consisted of two radiators: a square-ring patch and a square patch, which are both placed on a single-layer substrate with a dielectric constant of 2.65 and a square ground plane with an area of $100 \times 100 \text{ mm}^2$. For the square-ring patch antenna, its size is smaller than that of the conventional square and circular patch counterparts operated at the fundamental TM_{11} mode. Circular polarization of square-ring patch antennas can usually be achieved by feeding two detuned orthogonal signals. However, this dual-feeding mechanism has more complex geometry and larger size at the feeding network. A typical single-fed technique for producing a circular polarization wave involves the use

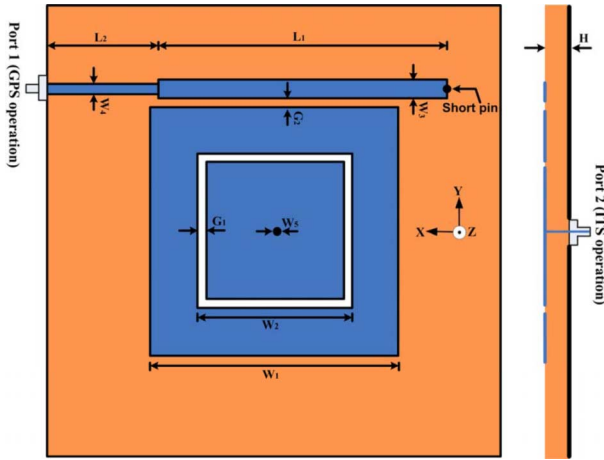


Fig. 1. Geometry of the proposed GPS/ITS integrated antenna.

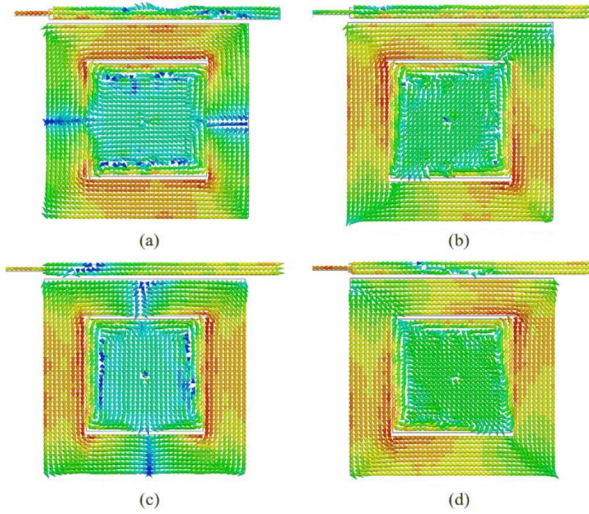


Fig. 2. Snapshots of the simulated current distribution of the proposed antenna at different phase values. (a) $\Delta\varphi = 0^\circ$. (b) $\Delta\varphi = 45^\circ$. (c) $\Delta\varphi = 90^\circ$. (d) $\Delta\varphi = 135^\circ$.

of a feeding structure to excite two closely degenerate resonant modes generated by truncating the corner of the square patch antenna [6] or inserting symmetrical perturbation strips [7].

In this letter, a novel coplanar capacitively coupled feeding structure is proposed to obtain circular polarization. The radiating outer square ring for GPS operation is proximity-coupling-fed by a parallel short-ended microstrip line. The coupling mechanism can be approximately considered as a microstrip coupled-line directional coupler. Port 1 for GPS operation excites energy on the microstrip line flowing from left to right (the short end), and it induces energy at the radiating square ring flowing from right to left (counterclockwise direction). This counterclockwise energy flow on the square ring works like a traveling-wave mode and contributes to a right-handed circular polarization. The simulated current distributions obtained from Ansoft High Frequency Structure Simulator (HFSS) shown in Fig. 2 can also be employed to explain the CP radiation. With the phase change, it can be observed that the maximum currents located at the azimuth angle turn in the counterclockwise direction, and the currents turn the x -axis into y -axis like an

TABLE I
DIMENSIONS OF THE PROPOSED ANTENNA (MILLIMETERS)

Parameter	H	W_1	W_2	W_3	W_4
Value	3	55	34	3	1
Parameter	W_5	L_1	L_2	G_1	G_2
Value	1.3	63	23	1	1.1

RHCP wave. This single-fed method is simple and flexible to obtain circular polarization without any alteration to the microstrip radiator such as truncating the corner and add-on slits. As a result, single-fed circular polarization could be achieved by only adjusting the microstrip feed lines, which is independent of the square-ring radiator. The impedance matching of integrated GPS antenna is affected by the intensity of the coupling, which is determined by the gap G_2 between square ring and the parallel short-ended microstrip line and the width W_3 .

ITS service requires an omnidirectional pattern with vertical polarization in the azimuth plane. More specifically, the radiated field has only θ -component and is invariable for all φ as monopole-like radiation pattern, which can ensure adequate coverage along low elevation planes. The conical TM_{02} mode of low-profile microstrip patch antennas with monopole-like radiation is a good candidate and has the advantage of a lower profile than the conventional quarter-wavelength monopole antenna. Nevertheless, the TM_{02} mode is a higher-order mode and has a high quality factor Q value and poor impedance matching. The coaxial probe feed to Port 2 for ITS operation is placed at the center of the inner square patch. In order to improve impedance matching, the outer square ring mentioned above is also utilized to load the center-fed square patch antenna. The loading technique with enhanced bandwidth is inspired by the annular-ring loaded (ARL) patch antennas [8]. The narrow slot between the outer square ring and the inner square patch can be modeled as π -type admittance network, and a dual resonance behavior is obtained to increase bandwidth. The impedance matching and optimum bandwidth of the integrated ITS antenna can be achieved by adjusting the width G_1 of the narrow slot and the probe diameter of W_5 . The notations and dimensions of the proposed antenna can be found in Table I.

The effect of the key geometrical parameters on the antenna performance has been studied. The other parameters were kept unchanged as the values in Table I when the influence of a particular parameter was investigated. The simulation software HFSS has been used in the study. As shown in Fig. 3, the variation of the W_1 does not change the reflection coefficient of the integrated ITS antenna much, but it is useful to tune the resonant frequency of the GPS band. The resonant frequency of the GPS antenna can be calculated according to the following [8]:

$$f = \frac{c}{2(W_1 + W_2)\sqrt{\epsilon_{\text{eff}}}} \quad (1)$$

where c is the speed of the light in the free space, $2(W_1 + W_2)$ is the mean circumference of the square-ring antenna, and ϵ_{eff} is the effective dielectric constant. Hence, shortening the width W_1 of the outer square ring will obtain the higher resonant frequency for Port 1. Fig. 4 shows the reflection coefficient for different width G_1 of the narrow slot. It is observed that the parameter G_1 will change the operating frequency and

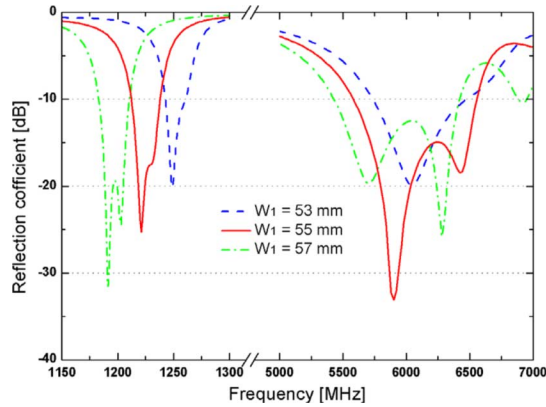


Fig. 3. Simulated reflection coefficient for different width W_1 of the outer square ring.

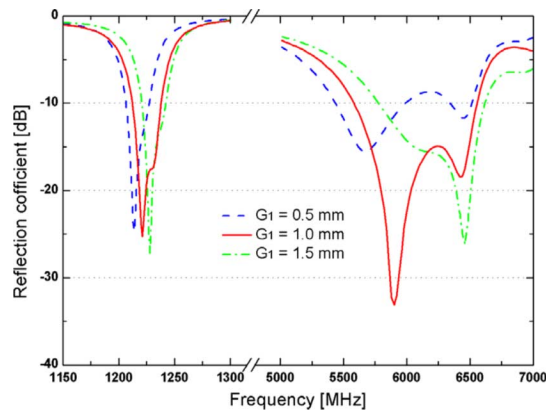


Fig. 4. Simulated reflection coefficient for different width G_1 of the narrow slot.

impedance matching of ITS band without affecting the GPS band too much. This is because the dual resonance behavior of the ITS band can be understood as exciting both the inner square patch and the outer square ring operating at the TM_{02} mode. As the slot width G_1 decreases, the resonant frequency will decrease by reason of increasing coupling between the inner square patch and the outer square ring. Moreover, the quality factor Q of the antenna decreases because of coupling, which results in a wide bandwidth. As mentioned, the coupling mechanism for circular polarization can be approximately considered as a directional coupler. Therefore, the coupling factor and phase relationship are influenced by the length L_1 of the short-ended microstrip line. As shown in Fig. 5, the length L_1 of the short-ended microstrip line can be tuned to obtain an optimum axial ratio for GPS operation after the impedance matching is achieved. The optimum axial ratio that can be achieved is about 0.32 at 1.228 GHz when the length L_1 of the short-ended microstrip line is 63 mm.

III. MEASUREMENT RESULTS

According to the parameters given in Table I, an antenna prototype was fabricated and measured. As shown in Fig. 6, the simulated values of the S_{11} and axial ratio for GPS operation are compared to the measured data. The measured data in general agree with the simulated results. The VSWR

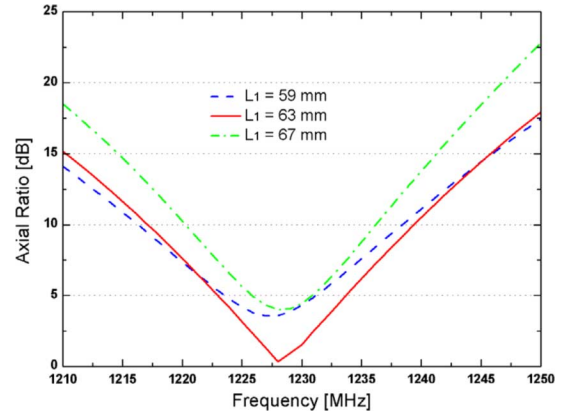


Fig. 5. Simulated axial ratio for different length L_1 of the short-ended microstrip line.

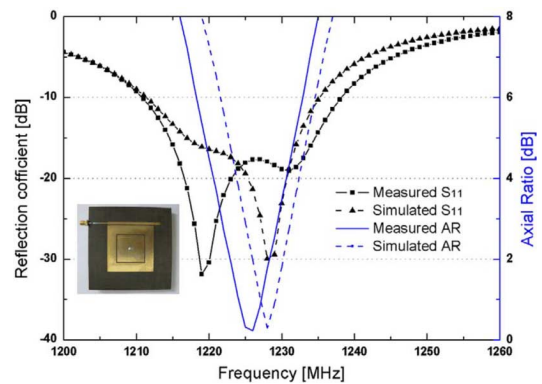


Fig. 6. Measured and simulated reflection coefficient S_{11} and axial ratio for GSP operation.

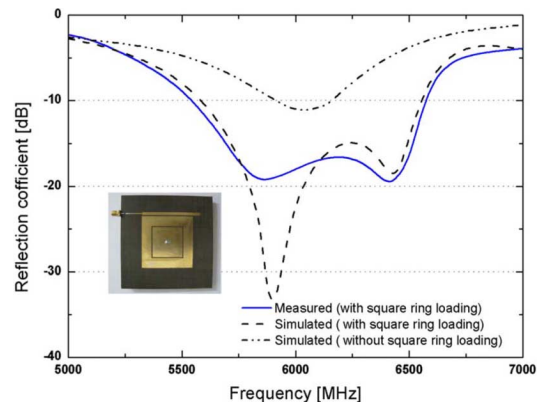


Fig. 7. Measured and simulated reflection coefficient S_{22} for ITS operation.

2:1 ($S_{11} < -10$ dB) impedance bandwidth is about 29 MHz (1210–1238 MHz), and 3-dB axial-ratio CP bandwidth is about 9 MHz around the center frequency of 1226 MHz. In addition, Fig. 7 shows the measured and simulated S_{22} for the integrated ITS antenna. It indicates that the measured impedance bandwidth of the proposed integrated ITS antenna with a height of only 3 mm ($<0.06\lambda$) is as large as 1020 MHz (5550–6570 MHz, 17.5%), while the reflection coefficient for the same one without square-ring loading is only -11 dB. The dual-resonance behavior of the square-ring loaded patch can be understood from the cavity mode.

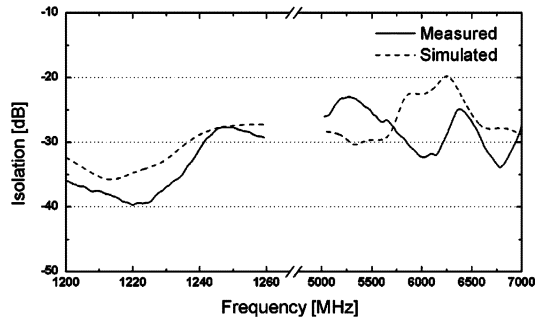


Fig. 8. Measured and simulated isolation between the feeding ports of GPS operation and ITS operation.

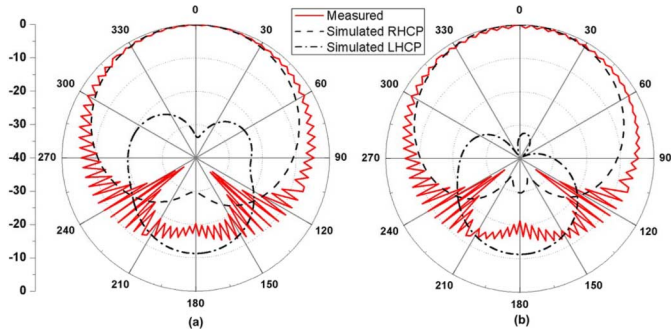


Fig. 9. Measured and simulated radiation patterns of the integrated GPS antenna at 1227 MHz. (a) xz plane. (b) yz plane.

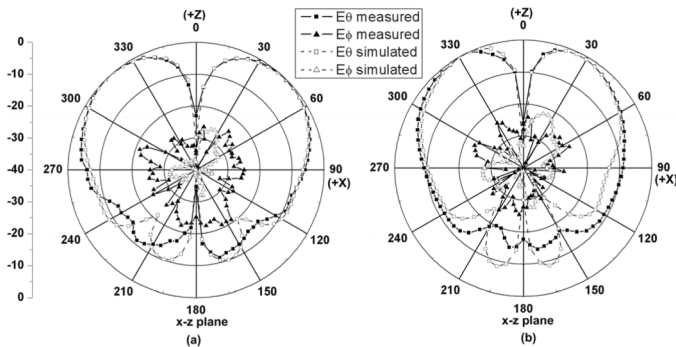


Fig. 10. Measured and simulated radiation patterns of the integrated ITS antenna. (a) 5.7 GHz. (b) 6.4 GHz.

Fig. 8 shows the measured and simulated isolation between the two feeding ports. High isolation (< -20 dB) for both GPS band and ITS band is achieved, showing that each integrated antenna operated correctly without significant interference from the other. Fig. 9 shows the radiation patterns of the integrated GPS antenna in both xz and yz planes at 1227 MHz with a spinning horn as the transmitting antenna. The peak and null of the zigzag curve in measured radiation pattern are the maximum and minimum record, respectively, when the spinning horn is rotated a circle. The magnitude of the ripple of the zigzag curve represents the purity of circular polarization. It is clear that a good right-handed CP radiation is observed. The measured and simulated radiation patterns of the proposed ITS antenna at different frequencies within the bandwidth are shown in Fig. 10. The measured radiation patterns coincide well with simulations. The copolarization patterns in the elevation plane are symmetrical, while the cross-polarization levels are about 20 dB below the copolarization. The measured and simulated antenna gain of

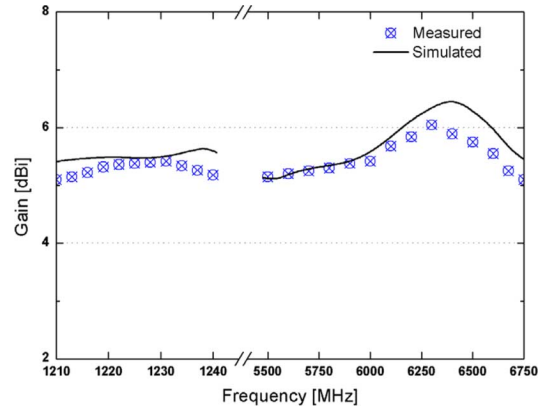


Fig. 11. Measured and simulated antenna gain of the multifunctional antennas.

the multifunctional antennas for operating frequencies are presented in Fig. 11. Over the bandwidth, the measured gain of the proposed ITS antenna varies between 5.1 and 6.1 dBi. In addition, the antenna peak gain of the proposed GPS antenna was found to be about 5.4 dBi.

IV. CONCLUSION

The design of a novel coplanar, collocated dual-port multifunctional antenna for dual-band operation (GPS/L2, ITS) with prescribed pattern and polarization was described in this letter. A coplanar simple single-fed method is proposed to obtain circular polarization without any alteration to the microstrip radiator, and it makes the microstrip feed lines independent of the square-ring radiator. Moreover, the square ring is also utilized to load the center-fed square patch antenna at TM_{02} mode with a vertical linear polarization for ITS application, which considerably increases the fractional bandwidth to 17.5% with a height of 3 mm only ($< 0.06\lambda$). The motivation for this work was to devise a novel solution for integrating different services into one multifunctional antenna with compact size and low-cost fabrication.

REFERENCES

- [1] Z. Zhang, M. F. Iskander, J. Langer, and J. Mathews, "Dual-band WLAN dipole antenna using an internal matching circuit," *IEEE Trans. Antennas Propag.*, vol. 53, no. 5, pp. 1813–1818, May 2005.
- [2] S.-Y. Lin and K.-C. Huang, "A compact microstrip antenna for GPS and DCS application," *IEEE Trans. Antennas Propag.*, vol. 53, no. 3, pp. 1227–1229, Mar. 2005.
- [3] *Standard Specification for Telecommunications and Information Exchange Between Roadside and Vehicle Systems 5 GHz Band Dedicated Short Range Communications (DSRC) Medium Access Control (MAC) and Physical Layer (PHY) Specifications*, ASTM 2213-03.
- [4] I. J. Garcia Zuazola, J. M. H. Elmirghani, and J. C. Batchelor, "Wimax antennas for intelligent transport system communications," in *Proc. Loughborough Antenna Propag. Conf.*, 2008, pp. 133–136.
- [5] G. H. Z. Rafi, M. Mohajer, A. Malarky, P. Mousavi, and S. Safavi-Naeini, "Low-profile integrated microstrip antenna for GPS-DSRC application," *IEEE Antennas Wireless Propag. Lett.*, vol. 8, pp. 44–48, 2009.
- [6] J. S. Row, "Design of square-ring microstrip antenna for circular polarization," *Electron. Lett.*, vol. 40, no. 2, pp. 93–95, Jan. 2004.
- [7] H.-M. Chen, Y.-K. Wang, Y.-F. Lin, C.-Y. Lin, and S.-C. Pan, "Microstrip-fed circularly polarized square-ring patch antenna for GPS applications," *IEEE Trans. Antennas Propag.*, vol. 57, no. 4, pp. 1264–1267, Apr. 2009.
- [8] T. Chakravarty, S. Biswas, A. Mujumdar, and A. De, "Computation of resonant frequency of annular-ring-loaded circular patch using cavity model analysis," *Microw. Opt. Technol. Lett.*, vol. 48, no. 3, pp. 622–626, Mar. 2006.